Electrochemical Measurements of Mass Transfer at Surfaces with Discrete Reactive Areas

Nikola M. Juhasz and William M. Deen
Dept. of Chemical Engineering, Massachusetts Institute of Technology, Cambridge, MA 02139

The limiting current technique was used to measure area-averaged mass-transfer coefficients for surfaces containing many small reactive areas arranged in various patterns. Partially masked platinum electrodes were fabricated using photolithography, and mass-transfer measurements were performed with a rotating disk apparatus. The average mass-transfer coefficient was sensitive to the fraction of the electrode area exposed (ϵ), declining from values near that for a fully exposed surface for $\epsilon = 0.5$ to less than 1% of the fully exposed value for $\epsilon = 0.001$. For any given ϵ, the mass-transfer coefficient declined with increased spacing between reactive sites. The results were relatively insensitive to details of the site distribution, such as whether the sites were arranged in regular arrays (square or hexagonal lattices) or distributed randomly over the surface. For all conditions studied, the mass-transfer coefficient greatly exceeded that predicted by conventional models which apply the stagnant film approximation to the fluid surrounding a representative active site. This finding is qualitatively consistent with recent computational results, which suggest that convective transport enhances mass transfer at partially active surfaces to an extent not accounted for by adjustments in the effective film thickness.

Introduction

A wide variety of processes involve surfaces which, on a small-length scale, are heterogeneous in terms of mass transfer. That is, chemical reaction or permeation is confined to numerous small reactive sites or pores, respectively, the remainder of the surface being unreactive or impermeable. Examples of such surfaces include supported catalysts, partially masked electrodes, and biological or synthetic membranes. To the extent that the overall rate of a process is limited by mass transfer in the fluid adjacent to such a heterogeneous surface, it is important to predict the value of the area-averaged mass-transfer coefficient. This averaged mass-transfer coefficient tends to be lower than that for a homogeneous (uniformly reactive or permeable) surface, because diffusional paths to or from discrete sites are longer on average.

The simplest and most commonly used theoretical models for mass transfer at heterogeneous surfaces assume that the active sites are equally spaced and focus on a "unit cell" centered on a single active site. If fluid flow is ignored, symmetry ensures that there is no mass transfer between adjacent unit cells, and a two-dimensional or axisymmetric diffusion problem is obtained (Dudukovic and Mills, 1985; Keller and Stein, 1967; Nanis and Kesselman, 1971; Reller et al., 1982; Smythe, 1953; Wakeham and Mason, 1979). Convective transport is often incorporated indirectly in such models by assuming that bulk fluid concentrations are reached at a specified distance from the surface. For a homogeneous surface, the thickness of this equivalent stagnant film must equal the solute diffusivity divided by the mass-transfer coefficient. If it is assumed that the same effective film thickness can be used for a heterogeneous surface under identical flow conditions, predictions of mass-transfer rates with a stagnant-film, unit-cell model only require knowledge of the mass-transfer coefficient for a homogeneous surface under the specified flow conditions, in addition to information on the size and spacing of active sites.

There have been only a few experimental investigations of mass transfer at well-characterized heterogeneous surfaces. One approach has been to measure diffusion through track-etch

Correspondence concerning this article should be addressed to W. M. Deen.
Present address of N. M. Juhasz: W. R. Grace & Co., Washington Research Center, Columbia, MD.

membranes of known pore size and pore number density (Beck and Schultz, 1972; Malone and Anderson, 1977; Bohrer, 1983). A difficulty with this approach is that the boundary-layer mass-transfer resistance must be determined by subtracting from the measured overall resistance the calculated resistance of the membrane pores. Also, the membrane fabrication process leads to pores which are distributed randomly over the surface, so that regular active site distributions cannot be studied. A second approach has been to employ partially masked, rotating disk electrodes (Scheller et al., 1968, 1969, 1970). In these systems, limiting currents can be used to provide a direct measurement of the boundary-layer resistance under well-defined hydrodynamic conditions, and a wide variety of site patterns can be produced using photolithography. As discussed previously in some detail (Juhasz and Deen, 1991), the various membrane and electrode results available to date have been inconsistent in their extent of agreement with predictions from the stagnant-film, unit-cell models.

The objective of this study was to obtain additional data with which to test the reliability of the existing unit-cell models. For the reasons already mentioned, we chose to employ partially masked electrodes in a rotating disk apparatus. The present results extend those of Scheller and coworkers by covering a wider range of geometric parameters. The most complete of the previous electrode studies (Scheller et al., 1970) used sites arranged in regular, rectangular arrays, with active area fractions (ϵ) in the range $0.06 \leq \epsilon \leq 1$. The present results include much smaller active area fractions ($0.001 \leq \epsilon \leq 1$) and encompass square, hexagonal and random arrays of sites.

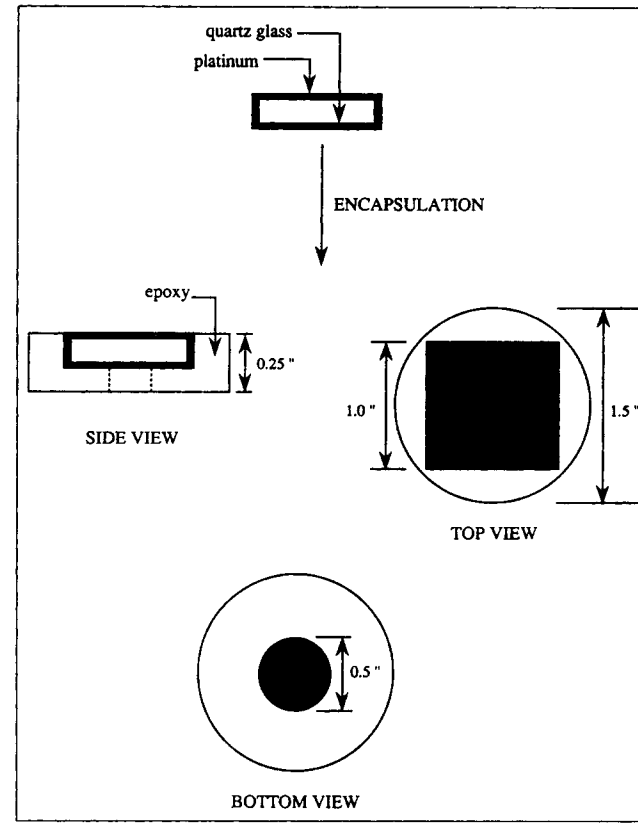

Figure 1. Electrode fabrication.

Square plates of glass were coated with platinum, encapsulated in epoxy, and the resulting disk machined to the dimensions shown.

Methods

Fabrication of partially masked electrodes

Partially masked electrodes were fabricated by an adaptation of photolithography techniques used in microelectronics processing. An electrically insulating polymeric photoresist was deposited onto a platinum electrode. Portions of the resist layer were then selectively removed by UV illumination through an overlaid mask and subsequent developing, thereby exposing the desired areas of the electrode. Further information on the electrode fabrication is given below. Additional details on these and other methods are available elsewhere (Juhasz, 1992).

Pieces [1 in.^{2} (645 mm^2)] of optically smooth glass (Nanofilm, Westlake Village, CA) were sputtered with platinum (Model 8620 Sputtering System, Materials Research Corporation, Orangebury, NY), to coating thicknesses of 0.1 μm on both flat surfaces. The metal layer was continuous around the edges, providing electrical continuity from the back to the front. Based on the resistivity of Pt, it was calculated that this coating thickness was sufficient to limit voltage drops in the Pt to $< 1\%$ of the applied voltage under all conditions studied. The coated glass pieces were then encapsulated in rigid epoxy disks, as shown in Figure 1. A circular cutout in the back of each disk allowed electrical contact to be made when it was mounted in the disk holder and rotator assembly. A thin film of epoxy (not shown in Figure 1) covered the periphery of the front surface of the electrode, leaving a more or less circular area exposed. The encapsulation and machining were performed by Pine Instrument Company (Grove City, PA).

The exposed surface of the epoxy-encapsulated electrode was spin-coated with a positive photoresist, KTI 820-20 (KTI Chemicals Inc., Sunnyvale, CA), at 4,000 rpm for 30 s, to produce a uniform 1.0 μm layer of resist on the surface. The thickness of the resist layer was sufficient to provide electrical insulation, while remaining much smaller than the dimensions of an active site. To obtain the desired surface pattern, the photoresist-coated disk was mounted on the alignment stage of a Karl Suss MJB 3 mask aligner (Karl Suss America, Inc., Waterbury Center, VT), and a chrome mask (see below) was centered directly atop the disk. The disk, with the overlaid mask, was then illuminated by ultraviolet light at 365 nm and 8 mW/cm^2 for 10 s. The exposed disk was developed in KTI 934 1:1 developer solution (KTI Chemicals) and rinsed in deionized water to remove the irradiated portions of the resist. An attractive feature of the patterning process was that the disks could be recycled simply by dissolving the photoresist layer with acetone and methanol. A given electrode could therefore be reused several times with different surface patterns.

Design and fabrication of masks

The masks used to transfer surface patterns to the electrodes contained clear features within opaque chrome backgrounds. The masks were generated using a computer-aided design utility, whereby a layout of the desired design was created and these data were then converted into a format which could be recognized by the mask generator (Pattern Generator 1005A, Gyrex Corp., Santa Barbara, CA).

Several patterns were designed with circular active sites ar-

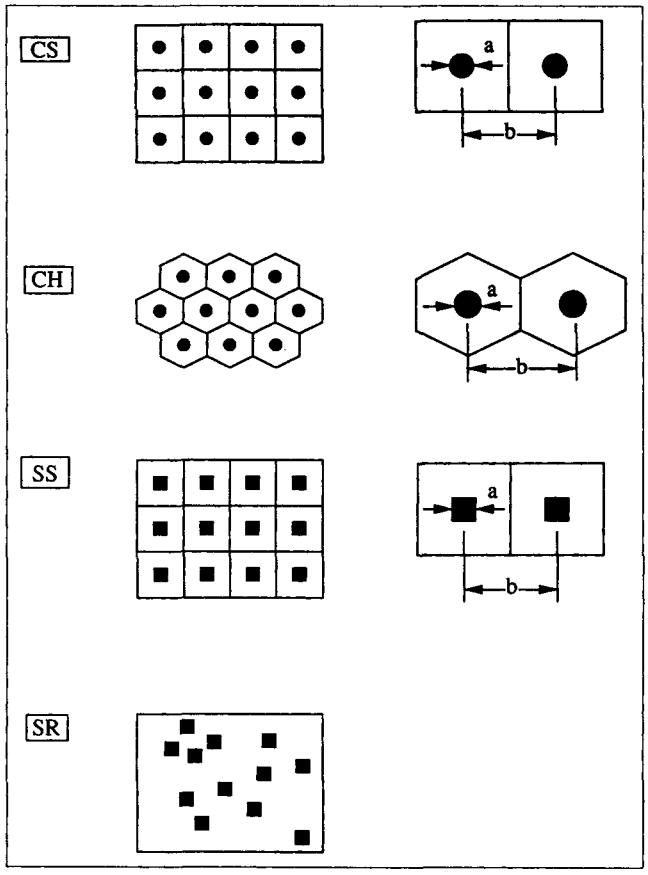

Figure 2. Types of patterns employed with partially masked rotating disk electrodes.

ranged on square lattices, that is, in square unit cells. These are designated by "CS" in Figure 2. The overall active area fraction for this geometry is $(\pi/4)(a/b)^2$, where a is the diameter of the active site and b is the length of a side of a unit cell or, alternatively, the site-to-site spacing. For a particular active site dimension and active area fraction, the distance between adjacent sites is given by $b = a\sqrt{\pi/(4\epsilon)}$. Another set of patterns was designed with circular active sites arranged in hexagonal unit cells (denoted by "CH"). The area of the hexagon in Figure 2 is $(\sqrt{3}/2)b^2$, where b is again the distance between adjacent active sites. Therefore, the active area fraction is $\epsilon = [\pi/(2\sqrt{3})](a/b)^2$. For a particular active site dimension, a, and active area fraction, ϵ, the site-to-site spacing is $b = a[\pi/(2\sqrt{3}\epsilon)]^{1/2}$. Square active sites were also employed in several patterns. For a square site/square array pattern ("SS"), the active area fraction is simply $\epsilon = (a/b)^2$. For a given active site dimension and active area fraction, $b = a/\sqrt{\epsilon}$.

In addition to the various regular patterns, square active sites in random arrays ("SR") were also studied. For each random pattern, coordinates on a 1 in. × 1 in. (25.4 mm × 25.4 mm) domain were produced by a random number generator (Marsaglia and Zaman, 1987) which required two seed values as inputs. Two calls to the routine produced a set of x-y coordinates in the domain. Successive sets of coordinates were checked against those previously accepted and rejected if any of the square sites overlapped. The process of generating and checking pairs of random numbers was repeated until the number of coordinates required to satisfy a particular active area fraction was obtained. To facilitate comparisons between random and regular site distributions, an average site-to-site spacing for the random patterns was defined as $b = a\sqrt{\epsilon}$ (as for a square lattice). Active site coverage for random arrays was restricted to low ϵ values.

Table 1. Electrode Patterns

Pattern	a (cm)	ϵ	b (cm)
CS1	0.040	0.005	0.50
CS2	0.040	0.01	0.36
CS3	0.040	0.05	0.16
CS4	0.040	0.1	0.11
CS5	0.040	0.5	0.050
CS6	0.010	0.001	0.28
CS7	0.010	0.005	0.13
CS8	0.010	0.01	0.088
CS9	0.010	0.05	0.040
CS10	0.010	0.1	0.028
CH1	0.010	0.001	0.30
CH2	0.010	0.005	0.13
CH3	0.010	0.01	0.096
CH4	0.040	0.05	0.17
SS1	0.010	0.05	0.045
SS2	0.010	0.5	0.014
SS3	0.0025	0.01	0.025
SS4	0.0025	0.05	0.011
SR1*	0.010	0.001	0.32§
SR2**	0.020	0.005	0.28§
SR3†	0.040	0.005	0.57§
SR4‡	0.040	0.01	0.40§

* Seed values input to random number generator were 1,752 and 100.
** Seed values input to random number generator were 150 and 100.
† Seed values input to random number generator were 1,500 and 1,700.
‡ Seed values input to random number generator were 3,010 and 2,481.
§ An average b value for random patterns was defined as $a/\sqrt{\epsilon}$ (see text).

The specific patterns employed are shown in Table 1. The active site dimensions ranged from 25 to 400 μm, always much larger than the 1 μm thickness of the resist. The fraction of the electrode area exposed in various patterns ranged from 0.001 to 0.5.

Electrochemical system

The reduction of ferri- to ferrocyanide, $Fe(CN)_6^{-3} + e^- \rightarrow Fe(CN)_6^{-4}$, was the reaction chosen for making mass-transfer measurements by the limiting current method. The usual practice with ferri/ferrocyanide solutions is to use large excesses of NaOH or KOH as a supporting electrolyte to suppress migration of the reacting ion (Selman and Tobias, 1978). However, because such alkaline solutions degrade the polymeric photoresist, the supporting electrolyte chosen was KCl. The solution composition employed was 0.01 M $K_3Fe(CN)_6$/0.01 M $K_4Fe(CN)_6$/1.0 M KCl, an equimolar concentration of ferri- and ferrocyanide in a large excess of KCl. The chemicals were all purchased from Sigma Chemical Company (St. Louis, MO).

Rotating disk apparatus

The experimental apparatus employed in making the limiting current measurements included a rotator (with disk holder and arbor assemblies), a set of three electrodes, a scanning poten-

tiostat, recording devices, and the electrochemical bath and receptacle. An AFASR Rotator and custom disk holder were obtained from Pine Instrument Company. The partially masked platinum disk electrode functioned as the working electrode in the system. A standard calomel reference electrode, (#RR1363952, Pine Instrument Company) was employed. A thin platinum sheet, approximately 2 in. × 2 in. (51 mm × 51 mm), served as the counterelectrode. The large surface area of this sheet ensured that the observed limiting current was due to reaction at the working electrode rather than at the counterelectrode. Both larger and smaller counterelectrodes were tested, with no detectable change in the limiting current readouts. Initial calibration studies were made with a commercially available platinum disk electrode (#AFDD20Pt, Pine Instrument Co.) functioning as the working electrode. This electrode had a circular platinum area of radius 0.382 cm. The electrodes were connected to a Model 362 Scanning Potentiostat from Princeton Applied Research (Princeton, NJ), and the current was monitored by a chart recorder and a digital multimeter connected through the potentiostat. A Pyrex container, 190 cm in diameter and 100 cm deep, was used for the electrochemical solution. These container dimensions exceed the minimum requirements described in literature reviews of rotating disk experiments (Gregory and Riddiford, 1956; Adams, 1969).

Experimental procedure

Limiting current measurements with each of the partially masked electrodes were made at rotation speeds of 100, 250, 500, 750 and 1,000 rpm. As the rotation rate was adjusted to the desired level, the potential was set to zero and the system was allowed to stabilize while a temperature reading was recorded. Then, a potential ramp (0 to 2.00 V at 10 mV/s) was applied and the resulting current was monitored on both the chart recorder and the multimeter. The limiting current value was indicated by a stable plateau in the plotted current vs. potential curve. An average value over the length of the plateau was recorded. The precision of a typical limiting current measurement was approximately ±5%. For any given electrode, the rotation speeds were selected in no particular order. Hysteresis effects were not observed. The complete set of readings at the five rotation speeds was repeated at least once, after a time interval ranging from 15 min to a few days.

Results

Preliminary experiments

An initial set of experiments was performed with the commercial electrode to confirm that the rotating disk system was behaving as expected. As derived by Levich (1962), the limiting current (i_L) for laminar flow at a uniform rotating disk is given by:

$$\frac{i_L}{mFAC_0} = 0.62 D^{2/3} \nu^{-1/6} \omega^{1/2} \qquad (1)$$

where m is the number of electrons transferred in the reaction, F is Faraday's constant, A is the disk area, C_0 is the bulk concentration of the reactant, D is the diffusivity of the reactant, ν is the kinematic viscosity, and ω is the angular velocity.

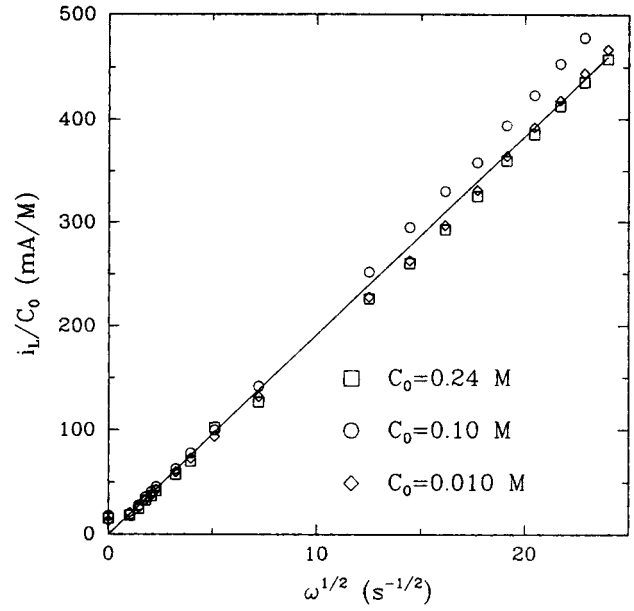

Figure 3. Limiting current data obtained in the rotating disk apparatus with a commercial platinum electrode.

The ratio of limiting current (i_L) to ferricyanide concentration (C_0) is plotted as a function of the angular velocity of rotation (ω). The symbols represent data at three values of C_0, whereas the line is the theoretical relationship from Eq. 1.

Note that $i_L/(mFAC_0)$ is equal to the mass-transfer coefficient (k_c). As shown in Figure 3, limiting currents measured at three bulk concentrations and a wide range of rotation rates were in good agreement with the line predicted by Eq. 1. Although there was reasonable agreement with Eq. 1 even at high ferricyanide concentrations (0.10 and 0.24 M), all subsequent experiments utilized the lowest concentration (0.01 M), as already noted. The values of D (for ferricyanide ion) at the measured temperatures of 20–25°C were obtained from Arvia et al. (1967).

A second set of tests was performed using three of the fabricated electrodes, but without any polymeric resist coating. For these particular electrodes, the area not covered by epoxy was exactly circular. This area was calculated directly from the measured diameter, and this result was compared with the value of A obtained from measurements of i_L and use of Eq. 1. A total of 15 comparisons (three electrodes at each of five speeds) yielded a root-mean-square difference between the two areas of 6.1%. This discrepancy is no greater than would be expected from the degree of precision of the limiting current readings and the diameter measurements. Thus, the fabricated electrodes, which were considerably larger than the commercial electrode, also showed no evidence of effects of finite container size or other nonidealities not accounted for by Eq. 1.

The effectiveness of the polymeric resist as an electrical insulator was tested by subjecting a fully coated (but not patterned) disk to potential ramps at the beginning and end of a two-hour immersion in the electrolyte solution and repeating this several days later. No current could be detected.

Partially masked electrodes

For each of the partially masked electrodes, the limiting

current (i_L) was compared with the limiting current measured for that same electrode in the absence of the polymeric resist (i_L^*). The current ratio i_L/i_L^* therefore equals the area-averaged mass-transfer coefficient for a given heterogeneous surface, divided by the area-averaged value for an otherwise identical homogeneous surface. Two of the important length scales in these experiments were defined in connection with Figure 2: the size of an active site (a) and the site spacing (b). The other important length scale is the thickness of the concentration boundary layer (δ). A convenient measure of δ is the diffusivity divided by the mass-transfer coefficient for a homogeneous surface. Accordingly, from Eq. 1,

$$\delta = \frac{D}{k_c} = 1.61\, D^{1/3} \nu^{1/6} \omega^{-1/2}. \tag{2}$$

If i_L/i_L^* is considered to be a function of a, b, and δ, then dimensional analysis indicates that only two ratios of these lengths are needed. We have chosen to express the results in terms of b/δ and the active area fraction, ϵ (determined by a/b).

A Peclet number representative of the conditions around an active site provides a measure of the importance of convection on that length scale. Choosing δ as the characteristic length and $\dot{\gamma}\delta$ as the characteristic velocity yields $Pe = \dot{\gamma}\delta^2/D$. As a representative surface shear rate, we chose $\dot{\gamma} = (\partial v_\theta/\partial z)_{z=0}$, where v_θ is the linear velocity in the direction of rotation and z is distance from the electrode surface. Thus, the velocity used ($\dot{\gamma}\delta$) roughly equals the rotational velocity (relative to the disk surface) at the outer edge of the concentration boundary layer. The similarity solution to the Navier-Stokes equations for a rotating disk (Levich, 1962) was used to evaluate $\dot{\gamma}$. (The order of magnitude of Pe would remain the same if the surface shear rate were based on the radial, rather than rotational, component of velocity.)

The values of ω, δ, $\dot{\gamma}$ and Pe for the conditions studied are shown in Table 2. Comparison of Tables 1 and 2 shows that the site spacing always exceeded the boundary layer thickness: that is, $b/\delta > 1$. Also, for the range of rotation rates which we found practical, Pe was always on the order of 10^3. Because Pe could not be varied independently of δ, Pe does not appear as a parameter in any of the plots.

All of the results for partially masked electrodes are shown in Figure 4. The symbols represent averages of two or more current measurements for a given rotation speed, and lines connect the five data points for any given pattern. Since b was fixed for a given electrode pattern, increasing the rotation speed increased b/δ, because of decreases in δ (Eq. 2). Two main trends are apparent. First, the normalized mass-transfer coefficient (normalized current) was very sensitive to the active area fraction, declining from values near unity for $\epsilon = 0.5$ to values lower than 0.01 for $\epsilon = 0.001$. Second, for any given ϵ, the mass-transfer coefficient declined with increasing b/δ, tending toward a constant value at high b/δ.

Table 2. Parameters Related to Rotation Rate of Disk Electrodes

ω (s^{-1})	δ (μm)	$\dot{\gamma}$ (s^{-1})	Pe
10.5	41.7	387.9	1,141
26.2	26.4	1,529	1,803
52.4	18.7	4,324	2,558
78.5	15.2	7,929	3,100
104.7	13.2	12,213	3,600

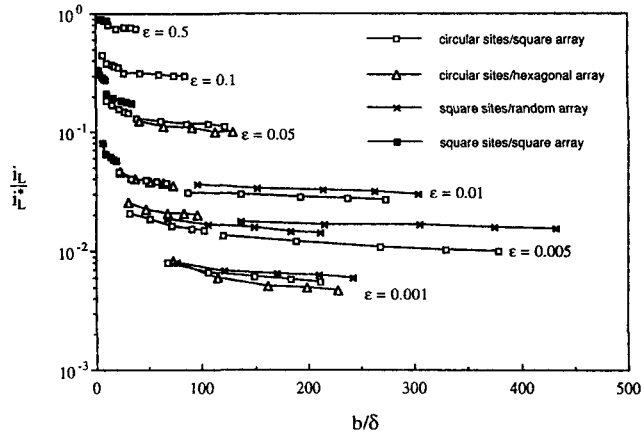

Figure 4. Limiting current data for all partially masked electrodes.

The limiting current for a given electrode (i_L) is normalized by that obtained for the same electrode without masking (i_L^*). The abscissa is the ratio of site spacing (b) to concentration boundary layer thickness (δ, see text). The fraction of exposed area (ϵ) is a parameter. Each group of five points connected by lines represents the average of at least two sets of measurements at each of five rotation rates with a given pattern.

In theory, as the site spacing becomes small relative to the concentration boundary layer thickness ($b/\delta \to 0$), the surface should eventually appear to be homogeneous (Keller and Stein, 1967; Juhasz and Deen, 1991). There is a suggestion of this behavior in Figure 4 at the smallest values of b/δ, although the minimum values of b/δ were not low enough to reach the limit $i_L/i_L^* = 1$ for any given pattern. In the opposite extreme of widely separated sites ($b/\delta \to \infty$ and $\epsilon \to 0$), one would expect the sites to act independently. An analysis based on a single circular site on a rotating disk (see Appendix) suggests that for widely separated sites,

$$\frac{i_L}{i_L^*} = 1.11\, \epsilon \left(\frac{R}{a}\right)^{1/3} \tag{3}$$

where R is the overall radius of the patterned area (in our case, the disk area not covered by epoxy). According to Eq. 3, the normalized current should become independent of rotation rate (or b/δ) at high b/δ, in agreement with the trends in Figure 4.

To provide a more quantitative comparison between the data and Eq. 3, we selected the eight patterns for which $\epsilon \le 0.01$ and $b/\delta > 200$ (at the highest rotation rate). Because the patterned areas usually were not exactly circular, R was calculated as the radius of a circle of equivalent area, with A determined from i_L^* using Eq. 1. When a given pattern was employed with two or more electrodes, the average value of i_L^* for the different electrodes was used to obtain an average R for that pattern. The results are shown in Table 3. The radius of the patterned areas was about 1 cm, and the standard deviations of i_L/i_L^* were 13% of the mean values on average. Some of the standard deviations probably underestimate the true uncertainty in i_L/i_L^*, especially when only one electrode was employed ($N = 2$).

Table 3. Comparison of Theoretical Predictions from Eq. 3 with Data for Widely Separated Active Areas

ϵ	Pattern	R (cm)	i_L/i_L^* (Data)*	i_L/i_L^* (Eq. 3)
0.01	CS2	0.72	$0.027 \pm 0.005(6)$	0.030
0.01	SR4	1.10	$0.030 \pm 0.009(6)$	0.034
0.005	CS1	0.95	$0.010 \pm 0.0001(4)$	0.016
0.005	SR2	1.14	$0.014 \pm 0.0003(2)$	0.021
0.005	SR3	1.12	$0.015 \pm 0.002(4)$	0.017
0.001	CS6	0.82	$0.0056 \pm 0.0015(6)$	0.0049
0.001	CH1	0.88	$0.0048 \pm 0.0001(2)$	0.0050
0.001	SR1	1.10	$0.0061 \pm 0.0007(4)$	0.0054

* The experimental values of i_L/i_L^* are for 1,000 rpm and are given as mean $\pm$S.D.(N), where N is the number of data points. The number of electrodes used with a given pattern was $N/2$.

The values of i_L/i_L^* from Eq. 3 were within 13% of the experimental values in six of the eight cases. Although Eq. 3 is strictly valid only for circular active areas, the extent of agreement was about the same with patterns involving circles or squares. Overall, the results in Table 3 support the use of Eq. 3 for low ϵ and high b/δ. The mass-transfer theory for a single circular site, on which Eq. 3 is based, is supported also by previous data obtained with 0.038 cm (Chin and Litt, 1972) or 0.64 cm (Mohr and Newman, 1975) diameter electrodes embedded in rotating disks.

The effects (if any) of the details of the site distribution were subtler than those of ϵ and b/δ. One comparison made involved square lattices with different diameters of active sites, $a = 0.01$ cm or 0.04 cm. The data for these patterns are replotted in Figure 5. The continuity of the pairs of curves for any given value of ϵ strongly suggests that there was no effect of site size at moderate values of b/δ. The absence of an effect of site size on the normalized mass-transfer coefficient is predicted by stagnant-film, unit-cell models for surfaces with interacting sites (Keller and Stein, 1967), in which the relative rate of mass transfer is determined only by ratios of the lengths a, b, and δ (see Discussion). For widely separated (noninteracting) sites, Eq. 3 indicates that i_L/i_L^* should vary as $(R/a)^{1/3}$. We were not able to test that prediction directly.

Other comparisons made included square vs. circular sites (with square lattices), square vs. hexagonal lattices (of circular sites), and square lattices vs. random distributions (of square sites). A close inspection of Figure 4 reveals modest differences among some curves in each of these categories. To assess the statistical significance of the differences, the same pattern was created on multiple plates and current measurements performed in duplicate on each, yielding typically 4-6 (and as many as 16) current vs. rotation rate curves for a given pattern. Variations between plates were usually greater than those between duplicate measurements with the same plate. Using an unpaired t test, there were significant differences at the 95% confidence level in the one comparison of square vs. circular sites, at one of four ϵ values with square vs. hexagonal lattices, and at one of three ϵ values involving square lattices vs. random distributions. Although statistically significant in a few instances, none of these differences seemed quantitatively important.

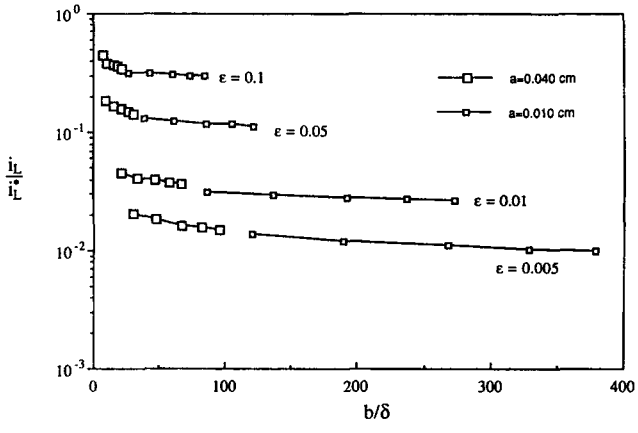

Figure 5. Limiting current data for "CS" electrodes having active sites of 0.040 or 0.010 cm diameter.
Other symbols are as in Figure 4.

Discussion

The main objective of these experiments was to evaluate the ability of existing theories to predict mass-transfer coefficients for heterogeneous surfaces. As already mentioned, the most common approach involves a calculation of purely diffusive transport in a single symmetry element (unit cell) centered on an active site. For circular sites within hexagonal (approximated as circular) unit cells, the solution to the axisymmetric diffusion problem was given by Keller and Stein (1967). In the present notation,

$$\frac{i_L}{i_L^*} = \frac{k_c}{k_c^*} = \frac{\epsilon}{4\alpha}\,\frac{1}{\phi(\alpha, \beta)} \tag{4}$$

$$\phi = \epsilon\left[\frac{1}{4\alpha} + \sum_{n=1}^{\infty} \frac{J_1^2(\gamma_n\alpha)\tanh(\gamma_n)}{(\gamma_n\alpha)^3 J_0^2(\gamma_n\beta)}\right] \tag{5}$$

where $\alpha = a/\delta$, $\beta = b/\delta$, $\epsilon = (a/b)^2$, and the eigenvalues (γ_n) are obtained from $J_1(\gamma_n\beta) = 0$. The electrode patterns that most closely approximated this situation were those involving circular sites in either hexagonal or square unit cells. Figure 6 shows a plot of the experimental values of i_L/i_L^* for all "CS" and "CH" patterns vs. the values of i_L/i_L^* predicted by the stagnant film model embodied by Eqs. 4 and 5. All points are well above the identity line, indicating that the mass-transfer coefficient is underestimated by the model. The amount of the underestimation is typically a factor of 2 to 5.

These results are qualitatively consistent with recent calculations of mass-transfer coefficients at heterogeneous surfaces for certain simple flows. For surfaces with equally spaced active stripes, area-averaged mass-transfer coefficients for laminar falling-film flow (Juhasz and Deen, 1991) or laminar tube flow (Juhasz and Deen, 1992) were found to depend on Pe, even in the fully developed mass-transfer region far downstream from the inlet. The ratio of the mass-transfer coefficient for a heterogeneous surface to that for a homogeneous surface followed the stagnant film predictions for low Pe, but began to significantly exceed the stagnant film values for $Pe > 10$. The reason for this is that convective transport parallel to the surface tended to smooth out the computed concentration variations between adjacent unit cells, thereby making the surface

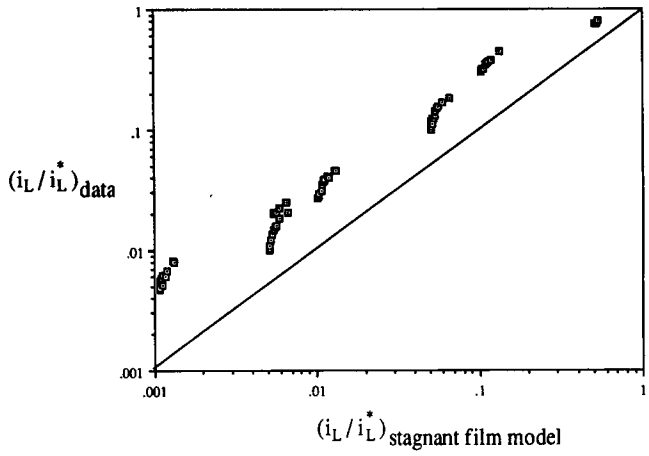

Figure 6. Normalized limiting current (i_L/i_L^*) measured with partially masked rotating disk electrodes, in comparison with values predicted by Eqs. 4 and 5.

The identity line is shown.

appear more homogeneous. These two-dimensional convective-diffusion calculations were limited to equally spaced active sites and to fully developed velocity and concentration fields. The results, however, do suggest that the stagnant film approach may systematically underestimate mass-transfer coefficients at heterogeneous surfaces for large *Pe*. As shown in Table 2, *Pe* in the present experiments ranged from 1,100 to 3,600. Values of this "microscale" Peclet number of 10 to 10^4 are typical of studies with rotating disks and stirred membrane diffusion cells (Juhasz and Deen, 1991).

The present results are also consistent in part with the findings of Scheller et al. (1970) using partially masked, rotating disk electrodes. From the information they reported, we calculated that b/δ for their experiments ranged from ~ 0.04 to ~ 4.0. We also determined that for their higher rotation rates, which yielded higher b/δ values most comparable to those employed here, their limiting currents exceeded those predicted by the stagnant film model. However, their measured currents at low values of b/δ (for which we have no data) were lower than the stagnant film predictions. Overall, we found that for their data the stagnant film calculations ranged from $\sim 80\%$ high at the lowest b/δ to $\sim 30\%$ low at the highest b/δ.

The results of mass-transfer studies using porous membranes in stirred cells do not show a clear pattern. Malone and Anderson (1977) found that Eqs. 3 and 4 correlated their data very well, in that a single value of δ could be chosen which fit results for membranes covering a range of ϵ. The value of δ for a homogeneous surface was not measured. Bohrer (1983), who measured δ for a homogeneous surface using the limiting current method, found that a much larger value of δ (by a factor of ~ 3) was needed for a membrane with low ϵ. In other words, Eqs. 3 and 4 overestimated k_c when δ for a homogeneous surface was used. Neither this finding nor the aforementioned results of Scheller et al. (1970) at low b/δ can be explained on the basis of the Peclet number, because the available two-dimensional calculations (Juhasz and Deen, 1991, 1992) suggest that the stagnant film model should tend to underestimate k_c. Bohrer (1983) suggested that the unexpectedly small experimental value of k_c might have been due to the random spatial distribution of pores. However, our comparisons of square lattices with random distributions showed little or no difference.

In conclusion, the present data show a tendency for the stagnant film model to underestimate the mass-transfer coefficient for a heterogeneous surface. This discrepancy is consistent with our previous suggestion (from two-dimensional computational results) that convective transport between active sites makes a surface appear more homogeneous than does the stagnant-film, unit-cell approach. Additional experiments seem to be needed to resolve the inconsistencies among various published studies. Additional convective-diffusion computations, involving three-dimensional concentration fields, might also be helpful in establishing correction factors (dependent on *Pe*) which could be applied to the stagnant film predictions.

Acknowledgment

Dr. Michael P. Bohrer of AT&T Bell Laboratories helped with pilot experiments, and the authors are grateful for his assistance and encouragement. Funding for equipment and supplies was provided by the MIT Department of Chemical Engineering. N. M. J. is the recipient of a graduate fellowship from the National Science Foundation.

Literature Cited

Adams, R. N., *Electrochemistry at Solid Electrodes*, p. 67, Marcel Dekker, New York (1969).

Arvia, A. J., S. L. Marchiano, and J. J. Podestra, "The Diffusion of Ferrocyanide and Ferricyanide Ions in Aqueous Solutions of Potassium Hydroxide," *Electrochim. Acta*, **12**, 259 (1967).

Bohrer, M. P., "Diffusional Boundary Layer Resistance for Membrane Transport," *Ind. Eng. Chem. Fundam.*, **22**, 72 (1983).

Chin, D.-T., and M. Litt, "Mass Transfer to Point Electrodes on the Surface of a Rotating Disk," *J. Electrochem. Soc.*, **119**, 1338 (1972).

Dudukovic, M. P., and P. L. Mills, "A Correction Factor for Mass Transfer Coefficients for Transport to Partially Impenetrable or Nonadsorbing Surfaces," *AIChE J.*, **31**, 491 (1985).

Gregory, D. P., and A. C. Riddiford, "Transport to the Surface of a Rotating Disc," *J. Chem. Soc.*, 3756 (1956).

Juhasz, N. M., "Mass Transfer at Heterogeneous Surfaces," PhD Thesis, Dept. of Chemical Engineering, MIT, Cambridge, MA (1992).

Juhasz, N. M., and W. M. Deen, "Effect of Local Peclet Number on Mass Transfer to a Heterogeneous Surface," *Ind. Eng. Chem. Res.*, **30**, 556 (1991).

Juhasz, N. M., and W. M. Deen, "Mass Transfer in a Tube with Wall Flux Confined to Evenly Spaced Discrete Areas," *Chem. Eng. Sci.*, **48**, 1745 (1992).

Keller, K. H., and T. R. Stein, "A Two-Dimensional Analysis of Porous Membrane Transport," *Math. Biosci.*, **1**, 421 (1967).

Levich, V. G., *Physicochemical Hydrodynamics*, pp. 60, 102, Prentice Hall, Englewood Cliffs, NJ (1962).

Malone, D. M., and J. L. Anderson, "Diffusional Boundary-Layer Resistance for Membranes with Low Porosity," *AIChE J.*, **23**, 177 (1977).

Marsaglia, G., and A. Zaman, *Toward a Universal Random Number Generator*, Florida State Univ., Report: FSU-SCRI-87-50, Tallahassee (1987).

Mohr, C. M., Jr., and J. Newman, "Mass Transfer to an Eccentric Rotating Disk Electrode," *J. Electrochem. Soc.*, **122**, 928 (1975).

Nanis, L., and W. Kesselman, "Engineering Applications of Current and Potential Distributions in Disk Electrode Systems," *J. Electrochem. Soc.*, **118**, 454 (1971).

Reller, H., E. Kirowa-Eisner, and E. Gileadi, "Ensembles of Microelectrodes: A Digital Simulation," *J. Electroanal. Chem.*, **138**, 65 (1982).

Rosner, D. E., "Reaction Rates on Partially Blocked Rotating Disks—

Effect of Chemical Kinetic Limitations," *J. Electrochem. Soc.*, **113**, 624 (1966).
Scheller, F., S. Müller, R. Landsberg, and H.-J. Spitzer, "Gesetzmässigkeit für den Diffusionsgrenzstrom an Teilweise Blockierten Modellelektroden," *J. Electroanal. Chem.*, **19**, 187 (1968).
Scheller, F., R. Landsberg, and S. Müller, "Zur Rührabhängigkeit des Grenzstromes an Teilweise Bedeckten Rotierenden Scheibenelektroden bei Relativ Grossen Underehungszahlen," *J. Electroanal. Chem.*, **20**, 375 (1969).
Scheller, F., R. Landsberg, and H. Wolf, "Über Kriterien für das Heterogene Verhalten von Electrodenoberflächen," *Z. Phys. Chem.*, **243**, 345 (1970).
Selman, J. R., and C. W. Tobias, "Mass-Transfer Measurements by the Limiting Current Technique," *Advances in Chemical Engineering*, Vol. 10, p. 211, T. B. Drew, G. R. Cokelet, J. W. Hoopes, Jr., and T. Vermeulen, eds., Academic Press, New York (1978).
Smyrl, W. H., and J. Newman, "Ring-Disk and Sectioned-Disk Electrodes," *J. Electrochem. Soc.*, **119**, 212 (1972).
Smythe, W. R., "Current Flow in Cylinders," *J. Appl. Phys.*, **24**, 70 (1953).
Wakeham, W. A., and E. A. Mason, "Diffusion Through Multiperforate Laminae," *Ind. Eng. Chem. Fundam.*, **18**, 301 (1979).

Appendix

In addition to the result for a uniform rotating disk (Eq. 1), laminar-flow mass-transfer analyses are available for certain types of partially active rotating disks. These include a disk with an annular active area (Levich, 1962; Rosner, 1966) and a ring-disk arrangement with an active central area and active annulus separated by an insulating annulus (Smyrl and Newman, 1972). Of particular interest here are results for a single, eccentrically positioned active spot (Chin and Litt, 1972; Mohr and Newman, 1975), which may be used to predict i_L/i_L^* for $\epsilon \to 0$. For a circular area of radius r_0 centered at a distance Er_0 from the axis of rotation, Mohr and Newman (1975) showed that for large E,

$$\frac{j}{j_{\text{disk}}} = 1.027 E^{1/3} \tag{A1}$$

where j is the rate of mass transfer (for example, mol·s^{-1}) at the eccentrically positioned area, and j_{disk} is the rate for a similar area undergoing axisymmetric rotation. A nearly identical result (with numerical coefficient smaller by 3%) was obtained by Chin and Litt (1972). In both cases, the results were obtained from two-dimensional convective-diffusion formulations which allowed for diffusion only in the direction normal to the disk surface. For such a formulation to be valid it is necessary that the concentration boundary layer which develops from the leading edge of the active area remains very thin relative to r_0. This requires in turn that the Peclet number based on the length r_0 and the velocity at the edge of the concentration boundary layer be very large. The Schmidt number must also be large.

If an electrode pattern contains n circular spots per unit area and if the spots are so widely separated that their effects are purely additive, then it follows from Eq. A1 that the area-averaged mass-transfer coefficient at a radial distance r from the axis of rotation is:

$$\frac{k_c(r)}{k_c^*} = 1.027 \epsilon \left(\frac{r}{r_0}\right)^{1/3} \tag{A2}$$

where k_c^* is the mass-transfer coefficient for a uniform rotating disk (Eq. 1). The area-averaged mass-transfer coefficient for the entire patterned area of radius R is:

$$\frac{\langle k_c \rangle}{k_c^*} = \frac{2}{R^2}\int_0^R \left(\frac{k_c}{k_c^*}\right) r\, dr = 0.880 \epsilon \left(\frac{R}{r_0}\right)^{1/3}. \tag{A3}$$

Using $r_0 = a/2$ and $\langle k_c \rangle / k_c^* = i_L/i_L^*$ in Eq. A3 leads to Eq. 3. The aforementioned requirement for large Peclet number indicates that this result should be valid asymptotically for $Pe \to \infty$, or alternatively, $b/\delta \to \infty$. The assumption that the spots act independently leads to the additional restriction that $\epsilon \to 0$.

Manuscript received Oct. 6, 1992, and revision received Mar. 18, 1993.